TISSUE ENGINEERING
Volume 11, Number 9/10, 2005

17)

Enhancement of Gap Junctional Intercellular Communication of Normal Human Dermal Fibroblasts Cultured on Polystyrene Dishes Grafted with Poly-*N*-isopropylacrylamide

TSUTOMU NAGIRA, Ph.D.,[1,2] SUSAN BIJOO MATTHEW, Ph.D.,[1] YOKO YAMAKOSHI, Ph.D.,[3] and TOSHIE TSUCHIYA, Ph.D.[1]

ABSTRACT

Technology developed to allow recovery of cells without enzyme treatment, involving a dish grafted with a thermoreactive polymer gel of poly-*N*-isopropylacrylamide (PIPAAm), was found to significantly enhance gap junctional intercellular communication (GJIC) in normal human dermal fibroblasts (NHDF cells). NHDF cells were cultured for 4 days on PIPAAm-grafted dishes irradiated with various doses of electron beams, and GJIC was assayed by the scrape-loading dye transfer method. The area of dye transfer was greater in the PIPAAm-grafted dishes than in the control culture dishes, indicating that the PIPAAm-grafted dishes enhanced the GJIC of NHDF cells. Connexin-43 (Cx43) expression was analyzed because Cx43 is considered to be a main component of the gap junctional channel. PIPAAm-grafted dishes irradiated with 100, 250, or 500 kGy of electron beams showed significantly enhanced expression of Cx43-NP, Cx43-P1, and especially Cx43-P2. Enhanced expression of Cx43-P2, a functional transmembrane protein, may be related to the promotion of GJIC. These results suggest that the PIPAAm-grafted dish not only enables the enzyme-free recovery of a cell monolayer for use in the construction of a three-dimensional artificial tissue, but also significantly contributes to the enhancement of GJIC, which may partly promote tissue strength on the surface of the PIPAAm-grafted dish.

INTRODUCTION

GAP JUNCTIONS exist on the cell membrane and work as intercellular channels that allow the exchange of substances with molecular masses up to 1 kDa, such as ions, sugars, and amino acids, by the function called gap junctional intercellular communication (GJIC).[1–3] Gap junctions are constructed from transmembrane proteins, called connexins,[4,5] that form a hemichannel, called a connexon. GJIC is suggested to be well correlated with passage of metabolites,[6] cell proliferation,[7] and cell differentiation[8]; thus, enhancement of the function of the gap junction is supposed to be important in the differentiation of engineered tissue products, such as those involving heart cells.[9–11] Poly-*N*-isopropylacrylamide (PIPAAm)-grafted dishes, which were originally developed as a thermosensitive scaffold for cell culture, are useful to maintain the GJIC of tissues cultured on them because they do not require enzyme treatment, which destroys connexins.[12–14]

PIPAAm is a thermoresponsive polymer that has a low critical solution temperature of 32°C: hydrated PIPAAm

[1]Division of Medical Devices, National Institute of Health Sciences, Tokyo, Japan.
[2]Japan Association for the Advancement of Medical Equipment, Tokyo, Japan.
[3]Center for Polymers and Organic Solids, Department of Chemistry and Biochemistry, University of California, Santa Barbara, Santa Barbara, California.

has an extended chain conformation below 32°C and dehydrated PIPAAm has a collapsed chain conformation above 32°C.[15–27] This property of PIPAAm has been exploited in intelligent materials for drug delivery systems and chromatography technology.[16–23] The PIPAAm-grafted dish has been found to enable the recovery of cell monolayers easily without enzyme treatment because cells cannot adhere to a hydrophilic surface below 32°C.[24–26] Cell monolayers are the basic units used to construct three-dimensional tissues *in vitro*. Because a cell monolayer recovered without enzyme treatment maintains normal adhesive and junctional proteins, it can easily adhere to the other tissues or cell sheets to construct a three-dimensional artificial tissue.[27–29] Thus, the PIPAAm-grafted dish has the potential to enable the development of new techniques in tissue engineering.

Although the PIPAAm-grafted dish has made a new era in tissue engineering possible, its effects on connexin-43 (Cx43) expression and GJIC have not been studied well. These effects are important because Cx43 plays an important role in cell proliferation and cell differentiation.

In this study, GJIC and expression of Cx43 molecules were examined by scrape-loading dye transfer (SLDT) assay[30] and Western blotting, respectively, using NHDF cells cultured on PIPAAm-grafted dishes irradiated with various doses of electron beams in order to clarify the safety and appropriateness of this material for the culture of artificial cultured tissues.

MATERIALS AND METHODS

Materials

N-isopropylacrylamide monomer (NIPAAm) was purchased from Wako Pure Chemical Industries (Osaka, Japan). Isopropyl alcohol was obtained from Dojindo (Kumamoto, Japan), and Lucifer yellow dye was from Molecular Probes (Eugene, OR).

Cell culture

Normal human dermal fibroblasts (NHDF cells; Sanko Junyaku, Tokyo, Japan) were cultured in Dulbecco's modified Eagle's medium (GIBCO DMEM; Invitrogen, San Diego, CA), supplemented with 10% heat-inactivated fetal calf serum (FCS; Invitrogen) and antibiotics (penicillin [100 units/mL]-streptomycin [100 units/mL]) (Invitrogen) at 37°C. NHDF cells were maintained in a humidified atmosphere of 5% CO_2 and 95% air.

Preparation of PIPAAm-grafted culture dishes

One hundred microliters of 40% NIPAAm dissolved in isopropyl alcohol was added to 35-mm dishes and irradiated with various doses of electron beams (25, 100, 250, or 500 kGy), using an area electron beam-processing system (Nissin High Voltage, Kyoto, Japan). The PIPAAm-grafted dishes were then rinsed three times with ice-cold sterile water (2 ml) for 5 min, sealed, and dried under vacuum.

Cell morphology

NHDF cells were cultured on control and PIPAAm-grafted dishes. Confluent cells (after 4 days of culture) were fixed with formalin solution, stained with 3% Giemsa solution, and observed with an optical microscope.

Protein assay

The protein concentration of cells cultured on control and PIPAAm-grafted dishes was measured with a bicinchoninic acid (BCA) protein assay kit (Pierce Biotechnology, Rockford, IL). Ten-microliter cell samples were

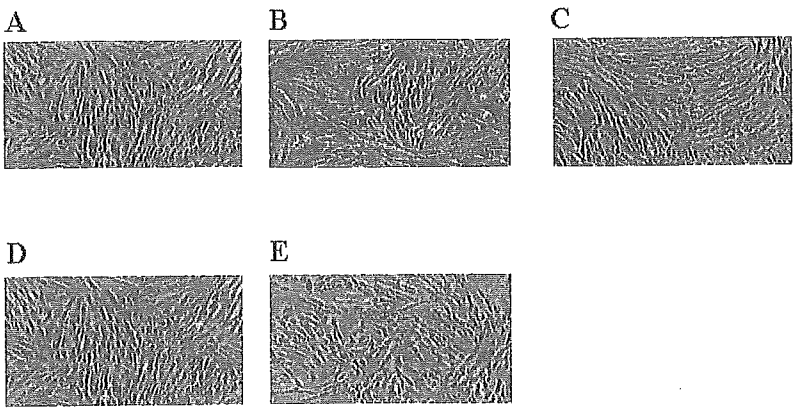

FIG. 1. Optical microscopy images of NHDF cells cultured on PIPAAm-grafted dishes. NHDF cells were cultured for 4 days on PIPAAm-grafted dishes prepared by irradiation with various doses of electron beams (0, 25, 100, 250, or 500 kGy). (**A**) Non-irradiated; (**B**) 25-kGy electron beam; (**C**) 100-kGy electron beam; (**D**) 250-kGy electron beam; (**E**) 500-kGy electron beam.

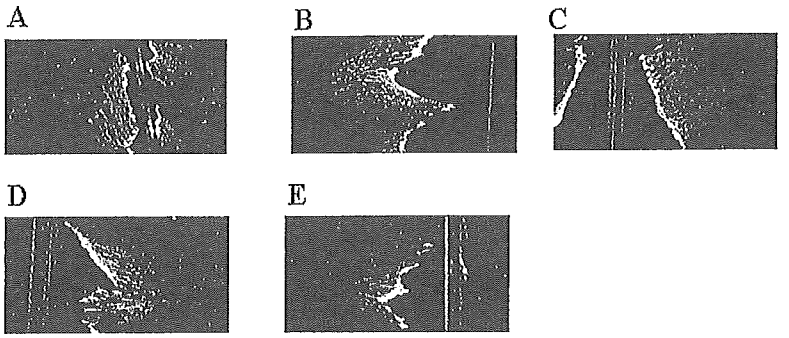

FIG. 2. Fluorescence of NHDF cells by SLDT assay. Transmission of Lucifer yellow into NHDF cells cultured on PIPAAm-grafted dishes irradiated with various doses of electron beams was detected 5 min after scrape-loading. (**A**) Nonirradiated; (**B**) 25-kGy electron beam; (**C**) 100-kGy electron beam; (**D**) 250-kGy electron beam; (**E**) 500-kGy electron beam.

added to 200 μL of the working solution and incubated at 37°C for 30 min in a 96-well plate. Absorbance was then measured at 562 nm in accordance with the manufacturer's protocols.

Scrape-loading dye transfer assay

NHDF cells were seeded on control and PIPAAm-grafted dishes at a density of 1×10^5 cells/mL and cultured for 4 days to form a confluent monolayer. Confluent NHDF cells were washed three times with phosphate-buffered saline containing Ca^{2+} and Mg^{2+} [PBS(+)], and the cell monolayer was scraped with a surgical blade. Fluorescent dye (Lucifer yellow; MW 457.2) at a concentration of 0.1% in PBS(+) was added.[30,31] Cells were exposed to the dye at 37°C for 5 min, and then the dye was discarded and the cells were washed four times with PBS(+). The distance that the dye had migrated was measured under a fluorescence microscope equipped with a type UFX-DXII CCD camera and super high-pressure mercury lamp power supply (Nikon, Tokyo, Japan). The dye migration was measured from the cut edge of the scrape to the edge of the dye front in the cells that were visually detectable.[30]

Western blotting

NHDF cells were cultured for 4 days. After being washed with ice-cold PBS(–) three times, the cells were lysed in 500 μL of lysis buffer (50 mM Tris-HCl [pH 6.8] containing 150 mM NaCl, 5 mM EDTA, 0.1 mM leupeptin, 1 mM phenylmethylsulfonyl fluoride, and 1% Nonidet P-40) for 30 min on ice with shaking. The cell lysates were centrifuged (10,000 rpm) at 4°C for 20 min, and the supernatants were collected. The protein concentrations of the lysates were determined by BCA assay.

Equivalent amounts of protein sample were applied to 12% sodium dodecyl sulfate (SDS)–polyacrylamide gels and then transferred to a nitrocellulose membrane at 120 V for 60 min. The membrane was blocked with Block Ace (Yukijirusi, Tokyo, Japan) overnight at 4°C. After being washed for 30 min in PBS with 0.05% Tween 20, the membrane was incubated for 2 h with anti-Cx43 polyclonal antibody [diluted 1:1000 in PBS(–) with 0.05% Tween 20; Zymed Laboratories, South San Francisco, CA], followed by incubation with horseradish peroxidase (HRP)-conjugated goat anti-rabbit IgG secondary antibody (diluted 1:5000; Zymed Laboratories). The image was visualized with an enhanced chemiluminescence (ECL) detection kit (Amersham Biosciences/GE Healthcare, Little Chalfont, UK).

Statistical analysis

Significant differences between groups were evaluated by Student t test. Mean differences were considered significant when $p < 0.05$.

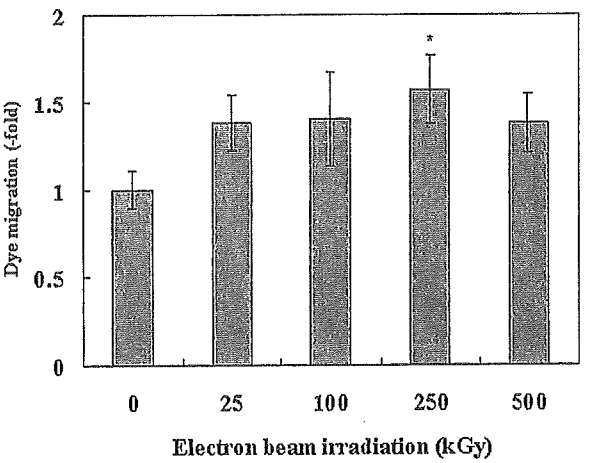

FIG. 3. Positive dye transfer in NHDF cells cultured on PIPAAm-grafted dishes. Transmission of Lucifer yellow was detected 5 min after scrape-loading in NHDF cells cultured on PIPAAm-grafted dishes irradiated with various electron beam doses (0, 25, 100, 250, or 500 kGy). Values represent means ± SD for three dishes. *Significant difference compared with control at $p < 0.05$ by t test.

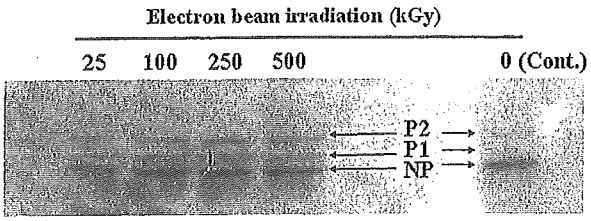

FIG. 4. Western blot of Cx43-NP, Cx43-P1, and Cx43-P2 expression; lysates of NHDF cells cultured on PIPAAm-grafted dishes irradiated with various doses of electron beams (0, 25, 100, 250, or 500 kGy) were applied to SDS–polyacrylamide gels. Fractionated proteins in the gels were transferred to nitrocellulose membrane and immunoblotted with anti-Cx43 polyclonal antibody as described in Material and Methods. Images of Cx43 on Western blot were captured with an Image scanner and analyzed with NIH Image software.

RESULTS

The appearance of NHDF cells grown on PIPAAm-grafted dishes irradiated with various doses of electron beams are shown in Fig. 1. No significant differences were observed by optical microscopy analysis between cells grown in dishes irradiated with various doses of electron beams. These results suggest that PIPAAm-grafted dishes are not toxic to NHDF cells.

The SLDT assay showed that dye migration in cells cultured on PIPAAm-grafted dishes irradiated with electron beams (25, 100, or 500 kGy) was enhanced by about 1.4-fold compared with that on control dishes. Interestingly, the dye migration in cells cultured on PIPAAm-grafted dishes irradiated with the 250-kGy electron beam was particularly enhanced, about 1.6 times higher than that on control dishes (Figs. 2 and 3). These results suggested that the GJIC of NHDF cells cultured on PIPAAm-grafted dishes was enhanced and that the GJIC on PIPAAm-grafted dishes irradiated with the 250-kGy electron beam was affected the most.

To further elucidate the effects of the PIPAAm grafting of culture dishes on GJIC, we analyzed the expression of Cx43, a transmembrane protein involved in GJIC. There are three forms of Cx43: Cx43-NP (nonphosphorylated Cx43), Cx43-P1 (monophosphorylated Cx43), and Cx43-P2 (another phosphorylated Cx43); Cx43-P2 is the most important and functional protein involved in GJIC. The results of Western blotting showed that the expression of Cx43-P1 and Cx43-P2 in NHDF cells cultured on PIPAAm-grafted dishes irradiated with 25, 100, 250, or 500 kGy of electron beams was considerably enhanced. Further, NHDF cells cultured on PIPAAm-grafted dishes irradiated with 100, 250, or 500 kGy of electron beams showed enhanced Cx43-NP expression (Figs. 4 and 5A). The Cx43-P2 expression of cells cultured on PIPAAm-grafted dishes irradiated with the 250-kGy electron beam dose showed the highest value, about 46% higher than that of control dishes. Cells cultured on PIPAAm-grafted dishes irradiated with electron beam doses of 25, 100, and 500 kGy were shown to have enhanced total Cx43 expression. Cells cultured on PIPAAm-grafted dishes irradiated with 100- and 250-kGy electron beam doses showed the highest total Cx43 expression, about 36.6% higher than that of control dish (Fig. 5B).

The Cx43-P2 expression of NHDF cells cultured on PIPAAm-grafted dishes irradiated with 25, 100, 250, and 500 kGy correlated well with GJIC ($R^2 = 0.9398$).

DISCUSSION

Thermoresponsive PIPAAm-grafted dishes irradiated with electron beams have been used to culture cell monolayers because the monolayers can be recovered without enzyme treatment, making PIPAAm a useful material for tissue engineering.

It has been reported that junctional proteins, cellular adherence proteins on the cell membrane, interact via

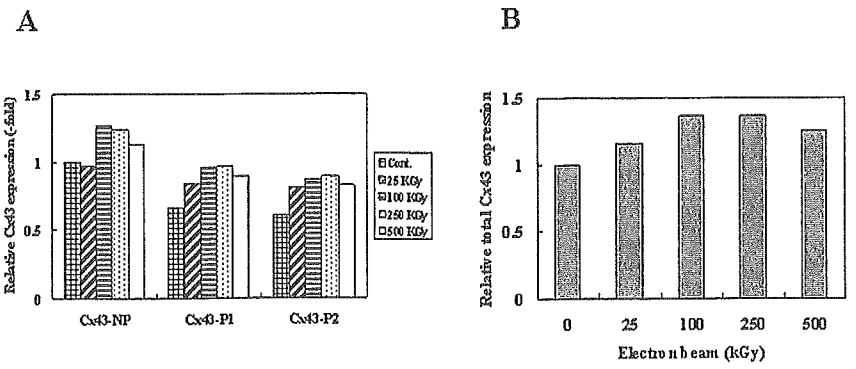

FIG. 5. Relative expression levels of Cx43-NP, Cx43-P1, and Cx43-P2 (A) and relative expression levels of total Cx43 (NP+P1+P2) (B) of NHDF cells cultured on PIPAAm-grafted dishes irradiated with various doses of electron beams (0, 25, 100, 250, or 500 kGy).

GJIC.[31] In this study, an SLDT assay demonstrated that dye migration in cultured NHDF cells was significantly enhanced in all PIPAAm-grafted dishes tested. Therefore, the chemical structure of the PIPAAm surface may stimulate junctional proteins on the cell membrane, and the stimulated junctional proteins may induce the enhancement of GJIC.

Cx43 expression of NHDF cells cultured on PIPAAm-grafted dishes irradiated with a 250-kGy electron beam changed significantly. Structural differences in PIPAAm triggered by the 250-kGy electron beam induced Cx43 protein expression by NHDF cells, probably by affecting the gene expression of NHDF cells. Further, total Cx43 expression was shown to be enhanced in cells cultured on PIPAAm-grafted dishes irradiated with various doses of electron beams (25, 100, 250, or 500 kGy). Differences due to the electron beam dose should be studied further.

Although the mechanism involved was not determined, it has been reported that basic fibroblast growth factor (bFGF) and keratinocyte growth factor (KGF) enhance GJIC activity and the expression of Cx43.[32–35] If bFGF and KGF in FCS are adsorbed onto the PIPAAm surface, cells can efficiently access these growth factors from the PIPAAm surface, and GJIC may be enhanced. It is also reported that bFGF activates protein kinase A (PKA),[36] an important regulator of Cx43, promoting the phosphorylation of Cx43 and enhancing GJIC.[37] Therefore, bFGF adsorbed onto the PIPAAm surface may bind its receptor and induce the activation of PKA, resulting in an enhancement of GJIC on NHDF cells caused by the increase in Cx43-P2 band protein.

In the process of posttranslational change, Cx43-P2 becomes insoluble in Triton X-100.[38] Thus, not all Cx43-P2 may be included in the lysate, and some Cx43-P2 may have been included in the pellet. More Cx43-P2 may have existed than was detected in the present results obtained by Western blotting.

In this study, it was shown that the use of PIPAAm-grafted dishes irradiated with various doses of electron beams enhanced GJIC and Cx43 expression in cultured NHDF cells. This suggests that PIPAAm-grafted dishes may promote efficient tissue regeneration, because GJIC plays an important role in increasing tissue strength.[39]

ACKNOWLEDGMENTS

This work was supported in part by a Grant-in-Aid for Scientific Research on Advanced Medical Technology from the Ministry of Labor, Health, and Welfare, Japan and by a Grant-in-Aid from the Japan Human Sciences Foundation.

REFERENCES

1. Giaume, C., Tabernero, A., and Medina, J.M. Metabolic trafficking through astrocyte gap junctions. Glia **21,** 114, 1997.
2. Abdullah, K.M., Luthra, G., Bilski, J.J., Abdullah, S.A. Reynolds, L.P., Redmer, D.A., and Grazul-Bilska, A.T. Cell-to-cell communication and expression of gap junctional proteins in human diabetic and nondiabetic skin fibroblasts. Endocrine **10,** 35, 1999.
3. Grossman, H.B., Liebert, M., Lee, I.W., and Lee, S.W. Decreased connexin expression and intercellular communication in human bladder cancer cells. Cancer Res. **54,** 3062, 1994.
4. Vera, B., Sanchez-Abarca, L.I., Bolanos, J.P., and Medina, J.M. Inhibition of astrocyte gap junctional communication by ATP depletion is reversed by calcium sequestration. FEBS Lett. **392,** 225, 1996.
5. Bukauskas, F.F., Jordan, K., Bukauskiene, A., Bennett, M.V., Lampe, P.D., Laird, D.W., and Verselis, V.K. Clustering of connexin 43–enhanced green fluorescent protein gap junction channels and functional coupling in living cells. Proc. Natl. Acad. Sci. U.S.A. **97,** 2556, 2000.
6. Giaume, C., Tabernero, A., and Medina, J.M. Metabolic trafficking through astrocytic gap junctions. Glia **21,** 114, 1997.
7. Tabernero, A., Jimenez, C., Velasco, A., Giaume, C., and Medina, J.M. The enhancement of glucose uptake caused by the collapse of gap junction communication is due to an increase in astrocyte proliferation. J. Neurochem. **78,** 890, 2001.
8. Tsuchiya, T. A useful marker for evaluating tissue-engineered products: Gap-junctional communication for assessment of the tumor-promoting action and disruption of cell differentiation in tissue-engineered products. J. Biomater. Sci. Polym. Ed. **11,** 947, 2000.
9. Giaume, C., Marin, P., Cordier, J., Glowinski, J., and Premont, J. Adrenergic regulation of intercellular communications between cultured striatal astrocytes from the mouse. Proc. Natl. Acad. Sci. U.S.A. **88,** 5577, 1991.
10. Warn-Cramer, B.L., Cottrell, G.T., Burt, J.M., and Lau, A.F. Regulation of connexin-43 gap junctional intercellular communication by mitogen-activated protein kinases. J. Biol. Chem. **273,** 9188, 1998.
11. Shimizu, T., Yamato, M., Isoi, Y., Akutsu, T., Setomaru, T., Abe, K., Kikuchi, A., Umezu, M., and Okano, T. Fabrication of pulsatile cardiac tissue grafts using a novel 3-dimensional cell sheet manipulation technique and temperature-responsive cell culture surfaces. Circ. Res. **22,** e40, 2002.
12. Nandkumar, M.A., Yamato, M., Kushida, A., Konno, C., Hirose, M., Kikuchi, A., and Okano, T. Two-dimensional cell sheet manipulation of heterotypically co-cultured lung cells utilizing temperature-responsive culture dishes results in long-term maintenance of differentiated epithelial cell functions. Biomaterials **23,** 1121, 2002.
13. Kushida, A., Yamato, M., Kikuchi, A., and Okano, T. Two-dimensional manipulation of differentiated Madin–Darby canine kidney (MDCK) cell sheets: The noninvasive harvest from temperature-responsive culture dishes and transfer to other surfaces. J. Biomed. Mater. Res. **54,** 37, 2001.
14. Shimizu, T., Yamato, M., Akutsu, T., Shibata, T., Isoi, Y., Kikuchi, A., Umezu, M., and Okano, T. Electrically com-

municating three-dimensional cardiac tissue mimic fabricated by layered cultured cardiomyocyte sheets. J. Biomed. Mater. Res. **60,** 110, 2002.
15. Takezawa, T., Mori, Y., and Yoshizato, K. Cell culture on a thermo-responsive polymer surface. Biotechnology **8,** 854, 1990.
16. Chung, J.E., Yokoyama, M., Yamato, M., Aoyagi, T., Sakurai, Y., and Okano, T. Thermo-responsive drug delivery from polymeric micelles constructed using block copolymers of poly(*N*-isopropylacrylamide) and poly (butylmethacrylate). J. Control. Release **62,** 115, 1999.
17. Chung, J.E., Yokoyama, M., and Okano, T. Inner core segment design for drug delivery control of thermo-responsive polymeric micelles. J. Control. Release **65,** 93, 2000.
18. Kurisawa, M., Yokoyama, M., and Okano, T. Gene expression control by temperature with thermo-responsive polymeric gene carriers. J. Control. Release **69,** 127, 2000.
19. Kobayashi, J., Kikuchi, A., Sakai, K., and Okano, T. Aqueous chromatography utilizing pH-/temperature-responsive polymer stationary phases to separate ionic bioactive compounds. Anal. Chem. **73,** 2027, 2001.
20. Kikuchi, A., and Okano, T. Pulsatile drug release control using hydrogels. Adv. Drug Deliv. Rev. **54,** 53, 2002.
21. Kanazawa, H., Sunamoto, T., Ayano, E., Matsushima, Y., Kikuchi, A., and Okano, T. Temperature-responsive chromatography using poly (*N*-isopropylacrylamide) hydrogel-modified silica. Anal. Sci. **18,** 45, 2002.
22. Kobayashi, J., Kikuchi, A., Sakai, K., and Okano, T. Aqueous chromatography utilizing hydrophobicity-modified anionic temperature-responsive hydrogel for stationary phases. J. Chromatogr. A **958,** 109, 2002.
23. Yoshizako, K., Akiyama, Y., Yamanaka, H., Shinohara, Y., Hasegawa, Y., Carredano, E., Kikuchi, A., and Okano, T. Regulation of protein binding toward a ligand on chromatographic matrixes by masking and forced-releasing effects using thermoresponsive polymer. Anal. Chem. **74,** 4160, 2002.
24. Kikuchi, A., Okuhara, M., Karikusa, F., Sakurai, Y., and Okano, T. Two-dimensional manipulation of confluently cultured vascular endothelial cells using temperature-responsive poly(*N*-isopropylacrylamide)-grafted surfaces. J. Biomater. Sci. Polym. Ed. **9,** 1331, 1998.
25. Kushida, A, Yamato, M., Konno, C., Kikuchi, A., Sakurai, Y., and Okano, T. Temperature-responsive culture dishes allow nonenzymatic harvest of differentiated Madin–Darby canine kidney (MDCK) cell sheets. J. Biomed. Mater. Res. **51,** 216, 2000.
26. Shimizu, T., Yamato, M., Kikuchi, A., and Okano, T. Two-dimensional manipulation of cardiac myocyte sheets utilizing temperature-responsive culture dishes augments the pulsatile amplitude. Tissue Eng. **7,** 141, 2001.
27. Hirose, M., Yamato, M., Kwon, O.H., Harimoto, M., Kushida, A., Shimizu, T., Kikuchi, A., and Okano, T. Temperature-responsive surface for novel co-culture systems of hepatocytes with endothelial cells: 2-D patterned and double layered co-cultures. Yonsei Med. J. **41,** 803, 2000.
28. Yamato, M., Utsumi, M., Kushida, A, Konno, C., Kikuchi, A., and Okano, T. Thermo-responsive culture dishes allow the intact harvest of multilayered keratinocyte sheets without dispase by reducing temperature. Tissue Eng. **7,** 473, 2001.
29. Harimoto, M., Yamato, M., Hirose, M., Takahashi, C., Isoi, Y., Kikuchi, A., and Okano, T. Novel approach for achieving double-layered cell sheets co-culture: Overlaying endothelial cell sheets onto monolayer hepatocytes utilizing temperature-responsive culture dishes. J. Biomed. Mater. Res. **62,** 464, 2002.
30. el-Fouly, M.H, Trosko, J.E., and Chang, C.C. Scrape-loading and dye transfer: A rapid and simple technique to study gap junctional intercellular communication. Exp. Cell Res. **168,** 422, 1987.
31. Defamie, N., Mograbi, B., Roger, C., Cronier, L., Malassine, A., Brucker-Davis, F., Fenichel, P., Segretain, D., and Pointis, G. Disruption of gap junctional intercellular communication by lindane is associated with aberrant localization of connexin43 and zonula occludens-1 in 42GPA9 Sertoli cells. Carcinogenesis **22,** 1537, 2001.
32. Pepper, M.S., and Meda, P. Basic fibroblast growth factor increases junctional communication and connexin 43 expression in microvascular endothelial cells. J. Cell. Physiol. **153,** 196, 1992.
33. Nadarajah, B., Makarenkova, H., Becker, D.L., Evans, W.H., and Parnavelas, J.G. Basic FGF increases communication between cells of the developing neocortex. J. Neurosci. **18,** 7881, 1998.
34. Park, J.U., and Tsuchiya, T. Increase in gap junctional intercellular communication by high molecular weight hyaluronic acid associated with fibroblast growth factor 2 and keratinocyte growth factor production in normal human dermal fibroblasts. Tissue Eng. **8,** 419, 2002.
35. Doble, B.W., and Kardami, E. Basic fibroblast growth factor stimulates connexin-43 expression and intercellular communication of cardiac fibroblast. Mol. Cell. Biochem. **143,** 81, 1995.
36. Pursiheimo, J.P., Jalkanen, M., Tasken, K., and Jaakkola, P. Involvement of protein kinase A in fibroblast growth factor-2-activated transcription. Proc. Natl. Acad. Sci. U.S.A. **97,** 168, 2000.
37. Faucheux, N., Zahm, J.M., Bonnet, N., Legeay, G., and Nagel, M.D. Gap junction communication between cells aggregated on a cellulose-coated polystyrene: Influence of connexin 43 phosphorylation. Biomaterials **25,** 2501, 2004.
38. Musil, L.C., and Goodenough, D.A. Biochemical analysis of connexin43 intracellular transport, phosphorylation, and assembly into gap junctional plaques. J. Cell Biol. **115,** 1357, 1991.
39. Gutstein, D.E., Morley, G.E., Tamaddon, H., Vaidya, D., Schneider, M.D., Chen, J., Chien, K.R., Stuhlman, H., and Fishman, G.I. Conduction slowing and sudden arrhythmic death in mice with cardiac-restricted inactivation of connexin43. Circ. Res. **88,** 333, 2001.

Address reprint requests to:
Toshie Tsuchiya, Ph.D.
Division of Medical Devices
National Institute of Health Sciences
1-18-1 Kamiyoga
Setagaya-ku, Tokyo 158-8501, Japan

E-mail: tsuchiya@nihs.go.jp

J Artif Organs (2005) 8:184–191
DOI 10.1007/s10047-005-0302-3

ORIGINAL ARTICLE

Nasreen Banu, MD · Yasmin Banu, MD, PhD
Masamune Sakai, BSc · Tadahiko Mashino, PhD
Toshie Tsuchiya, PhD

Biodegradable polymers in chondrogenesis of human articular chondrocytes

Abstract The aim of this study was to evaluate the potential role of polyglycolic acid (PGA), poly(glycolic acid-ε-caprolactone) (PGCL), poly(L-lactic acid-glycolic acid) (PLGA), poly(L-lactic acid-ε-caprolactone, 75:25 (w/w)) [P(LA-CL)25], poly-ε-caprolactone (tetrabutoxy titanium) [PCL(Ti)], and fullerene C-60 dimalonic acid (DMA) in cartilage transplants. After 4 weeks of culture of human articular cartilage, the levels of cell proliferation and differentiation and the expression of cartilage-specific matrix genes were estimated. The relationship between cell differentiation and gap junction protein connexin 43 (Cx43) was also evaluated. All materials except PCL(Ti) retained cell proliferation activities similar to the controls. Cell differentiation levels from the highest to the lowest were in the following order: PGA >> PLGA > PGCL > Control = DMSO > P(LA-CL)25 = PCL(Ti) >> fullerene C-60 DMA. Expression of the collagen type II gene was selectively upregulated for PGA, PGCL, and PLGA and slightly increased for P(LA-CL)25 polymers but was downregulated for fullerene C-60 DMA. Aggrecan gene expression was strongest with PGA and was consistently expressed with other matrices, especially with PGCL and PLGA. However, the expression patterns of the connexin 43 gene were different from the former two genes. Multiple regression analysis revealed a high correlation between cartilage proteoglycans production and expression levels of these three genes.

Key words Human articular chondrocytes · Biodegradable polymers · Matrix gene · Connexin 43

Received: February 2, 2005 / Accepted: June 8, 2005

N. Banu · Y. Banu · T. Tsuchiya (✉)
Division of Medical Devices, National Institute of Health Sciences,
1-18-1 Kamiyoga, Setagaya-ku, Tokyo 158-8501, Japan
Tel. +81-3-3700-9196; Fax +81-3-3700-9196
E-mail: tsuchiya@nihs.go.jp

M. Sakai
Polymer Laboratory, UBE Industries, Ltd., Chiba, Japan

T. Mashino
Kyoritsu University of Pharmacy, Tokyo, Japan

The first two authors contributed equally to this work

Introduction

A shortage of donor tissue restricts the successful application of tissue reconstruction for various cartilage injuries. Tissue engineering is a relatively new and promising field directed at the evolution of new tissues that will offer hope to orthopedic patients with a variety of injuries. To permit repair of cartilage defects, many researchers are turning toward a tissue engineering approach involving cultured cells and biomaterials. Although these biomaterials, especially polyglycolic acid (PGA) and poly(L-lactic acid) (PLLA), play an increasingly important role in orthopedics, adverse reactions to these biomaterials have been reported in animal experiments. PLLA produces toxic substances due to acidic degradation,[1] and long-term implants of PLLA produced tumorigenicity in rats.[2] Despite these setbacks, numerous studies have documented the biocompatibility of these bioabsorbable polymers.[3–7] PLLA, PGA, and their copolymers also have been used in clinical practice.[5,8] More recent studies have indicated that copolymers of glycolic acid promoted peripheral nerve regeneration in a rat model.[9,10] These polymers are degraded by hydrolysis and enzymatic activity and have a range of mechanical and physical properties that can be engineered appropriately to suit a particular application.

Knowledge of the biological interactions between chondrocytes and biodegradable polymers is needed to design novel biomaterials and to develop new strategies for cartilage repair. Therefore, further experimental elucidation of these polymers, their combination with other biomaterials, and new materials to find good substrates is essential to attain satisfactory conditions for their clinical application. In this study, along with PGA and poly(L-lactic acid-glycolic acid) (PLGA), we investigated the copolymer poly(glycolic acid-ε-caprolactone) (PGCL), the copolymer poly(L-lactic acid-ε-caprolactone) 75:25 (w/w) P(LA-

CL)25, and poly-ε-caprolactone (tetrabutoxy titanium) [PCL(Ti)] to determine their effects on human articular chondrocyte (HAC) proliferation, differentiation, and phenotypic expression with the aim of clarifying their suitability as carriers for future clinical cartilage transplants. Fullerene C-60 dimalonic acid (DMA) has been reported to stimulate[11] and inhibit[12] proliferation and differentiation of rat embryonic limb bud cells and mouse embryo midbrain cells, respectively, and in the present study we also investigated the effect of fullerene C-60 DMA on HACs.

Gap junctions are intercellular channels supporting direct cell-to-cell communication and tissue integration.[13] Connexins, the family of proteins that form vertebrate gap junctions, play key roles during development and in the adult. Among the 19 connexins that have been identified in mammals, the gap junction protein connexin 43 (Cx43) is the most abundant member of the channel-forming proteins in chondrocytes.[14,15] The distribution of Cx43 in hyaline cartilage and in the perichondrium of mouse and rat knee joints suggested a possible involvement of connexins in cartilage development.[16] It has been indicated that the early stage of in vitro chondrocyte differentiation is the formation of cell condensations and the ability to establish cell-to-cell communication. Cx43, together with other molecular mechanisms, mediates the condensation phase of chondrogenesis.[17] In the present study, we investigated the role of gap junctional protein Cx43 in the process of chondrocyte differentiation.

Materials and methods

Materials

HACs from knee joints and chondrocyte growth medium were commercially obtained from BioWhittaker (Walkersville, MD, USA). Chondrocyte growth medium contains bovine insulin, basic fibroblast growth factor, insulin-like growth factor-1, transferrin, gentamicin sulfate, and fetal bovine serum (5% v/v). PGA (mw 3000) and PLGA (mw 5000) were purchased from Nakalai Tesque (Kyoto, Japan) and PGCL (mw 3000) was from Taki Chemical (Hyogo, Japan). P(LA-CL)25 (mw 10000) and PCL(Ti) (mw 130000) were synthesized in our laboratory and fullerene C-60 DMA was obtained from Dr. T. Mashino.[18]

Synthesis of P(LA-CL)25

L-Lactide (Tokyo Kasei Kogyo, Tokyo, Japan) 7.5 g and caprolactone (Wako Pure Chemical Industries, Osaka, Japan) 2.5 g were put into a reactor as monomers. As a catalyst, tetrabutoxy titanium (Wako) 0.03 g was added. Furthermore, *n*-octyl alcohol (Wako) 0.001 g was added. These were completely dissolved in methylene chloride (Wako) 50 mL at room temperature. Methylene chloride was removed by decompression and a uniform mixture was left. The reactor was filled with nitrogen and was sealed. The contents were mixed and heated to 140°C. Polymerization was carried out for 4 h. After the reaction, the reactant was cooled to room temperature, and was dissolved in tetrahydrofuran 100 mL. The solution was dropped into cold methanol and a colorless precipitate was obtained. This was dried under reduced pressure and precipitation was done once again. This was again dried under reduced pressure and the polymer was obtained. The yield was 58.2% (5.82 g).

Synthesis of PCL(Ti)

Synthesis was done using the same method as described for the synthesis of P(LA-CL)25 except that the monomer was only caprolactone (Wako). The yield was 87.1% (8.71 g).

Preparation of materials

PGA, PGCL, PLGA, and P(LA-CL)25 were dissolved in dimethyl sulphoxide (DMSO) at a concentration of 50 μg/0.8 μl of DMSO (Sigma-Aldrich, Irvine, CA, USA) and then dissolved in chondrocyte growth medium to give a final concentration of 50 μg/ml. PCL(Ti) was dissolved in tetrahydrofran (THF) at a concentration of 5 mg of PCL/ml of THF. Glass wells were coated with this solution to give a final concentration of 2 mg PCL(Ti)/well. A homogenous solution of fullerene C-60 DMA was made with the chondrocyte growth medium.

Cell culture

In vitro high-density micromass cultures of HACs were initiated by spotting 4×10^5 cells in 20 μl of medium onto each well of 12-well microplates for tissue culture (Costar Type 3513, Corning, Corning, NY, USA) and PCL(Ti)-coated glass wells (diameter 22 mm). After 2 h in a 5% CO_2 incubator at 37°C, the wells were flooded with chondrocyte growth medium (2 ml/well). The medium was supplemented with DMSO (0.8 μl/ml), PGA (50 μg/ml), PGCL (50 μg/ml), PLGA (50 μg/ml), P(LA-CL)25 (50 μg/ml), or fullerene C60 DMA (50 μg/ml). HACs cultured on tissue culture polystyrene but not exposed to any biomaterials served as a control. The media were changed in every 3 days and culture was continued for 4 weeks.

Cell morphology assay

Cell morphology was determined by inverted light microscopy. Twice weekly observations were done and photographs were taken with Fuji film.

Proliferation assay

Cell proliferation was quantitatively measured by alamar blue (Biosource International, Camarillo, CA, USA) assay after 4 weeks of culture, as previously described.[18] The assay

demonstrates the metabolic activity of the cells by detection of mitochondrial activity. The indicator dye alamar blue is incorporated into the cells and reduced and excreted as a fluorescent product. At the end of the 4-week culture period, the medium from all wells was discarded and the culture wells and three blank wells were filled with 1 ml/well of 5% alamar blue solution in fresh medium. The culture plates were incubated at 37°C for 4 h. After the incubation period, two aliquots of 100 µl of solution from each well were transferred to new wells of a Costar 96-well tissue culture microplate (Costar Type 3595, Corning). The extent of cell proliferation was quantitated by a Cytofluor II fluorescence multiwell cell reader (PerSeptive Biosystems, Framingham, MA, USA) at 535 nm for excitation and 590 nm for emission. The intensity of the blue color obtained was directly proportional to the metabolic activity of the cell populations. Blank values were subtracted from experimental values to eliminate background readings.

Proteoglycan production assay

Proteoglycans are typical components of the cartilage matrix. The extent of chondrogenesis was determined by staining the cartilage-specific proteoglycans with alcian blue (Wako) as described previously.[11,19] Briefly, the cultures and three blank wells were stained overnight at 4°C (0.5 ml/well) with 1% (v/v) alcian blue, pH 1.0. The alcian blue solution was then removed and the micromass cultures and blank wells were rinsed with 3% (v/v) acetic acid and distilled water to completely remove the free dye. The cartilage proteoglycans were extracted using 4-M guanidine hydrochloride, and the absorbance was measured at a wavelength of 600 nm using an enzyme-linked immunosorbent assay (ELISA) reader (Bio-Tek Instruments, Winooski, VT, USA). Blank values were subtracted from experimental values to eliminate background readings.

RNA harvest

After the 4-week culture period, RNA was extracted from all matrices except the PCL(Ti) matrix. For the PCL(Ti) matrix, we did not have enough samples to harvest RNA because cells from 50% of the cultured wells became detached overnight following cell spotting. Total cellular RNA was extracted from cultured cells of four wells (for each material) in 0.5 ml Trizol reagent (Life Technologies, Frederick, MD, USA) according to the manufacturer's instructions. The concentration of total RNA was determined using a UV spectrophotometer (Gene Quanta, Pharmacy Biotech, Piscataway NJ, USA) at 260 nm.

Reverse transcription (RT) and polymerase chain reaction (PCR)

The matrix molecules probed as part of this study were collagen type II and aggrecan. The gap junction protein gene Cx43 was also studied. Single-strand cDNA was prepared from 1 µg of total RNA by reverse transcription (RT) using a commercially available First-Strand cDNA synthesis kit (Amersham Pharmacia Biotech, Uppsala, Sweden). After optimization of PCR conditions, subsequent PCR was performed with 4 µg of cDNA in a 20-µl reaction mixture (10 × PCR buffer 2 µl, dNTP 1.6 µl, forward and reverse primer 0.4 µl, Taq DNA polymerase 0.1 µl, and distilled water to make up 20 µl). The codon sequence used for the primer sets was as follows:

Collagen type II:
forward 5′-GGCAATAGCAGGTTCACGTACA-3′
reverse 5′-CGATAACAGTCTTGCCCCACTT-3′

Aggrecan:
forward 5′-TCGAGGACAGCGAGGCC-3′
reverse 5′-TCGAGGGTGTAGCGTGTAGAGA-3′.

Connexin 43 (*Homo sapiens*):
forward 5′-ATGGGTGACTGGAGCGCCTTAGGCAAACTC-3′
reverse 5′-GACCTCGGCCTGATGACCTGGAGATCTAG-3′

For collagen type II and Cx43, an initial denaturation step at 94°C was carried out for 5 min, followed by 40 cycles of 94°C for 1 min, 60°C for 1 min, and 72°C for 1 min, with a final extension at 72°C for 10 min. For aggrecan, an initial denaturation at 95°C was carried out for 10 min, followed by 40 cycles of 95°C for 15 s, 60°C for 1 min, and 72°C for 1 min), with a final extension at 72°C for 5 min. The polymerization of glyceraldehyde-3-phosphate dehydrogenase (GAPDH) was accomplished by 25 cycles with a corresponding PCR program. Electrophoresis of PCR products was done on 3% agarose gel for visualization of collagen type II and aggrecan and on 1% agarose gel for Cx43 after staining with SYBR Green I (BioWhittaker Molecular Applications, Rockland, ME, USA). The relative intensity of signals from each lane was analyzed with a computerized scanner. For relative quantitation, the signal intensity of each lane was standardized to that of a housekeeping gene, GAPDH:

forward 5′-CCCATCACCATCTTCCAGGAGCGAGA-3′
reverse 5′-TGGCCAAGGTCATCCATGACAACTTTGG-3′.

Statistical analysis

Comparing the control with samples exposed to various materials assessed the statistical significance of the cell proliferation and cartilage proteoglycans production. Student's *t* test was used to assess the statistical significance. Statistical significance was taken as $P < 0.05$. Data were indicated as the mean ± SD (standard deviation). Four or five cultures were run for each biomaterial. All experiments were repeated at least twice, and similar results were obtained.

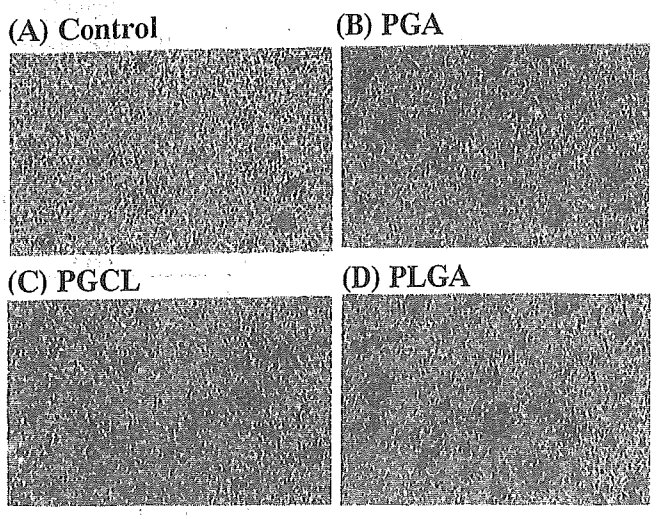

Fig. 1A–D. Light microscopic appearance of cultured human articular chondrocytes spotted as a high-density micromass culture with different biodegradable polymers for 4 weeks. **A** Control, **B** polyglycolic acid (PGA), **C** poly(glycolic acid-ε-caprolactone) (PGCL), **D** poly(L-lactic acid-glycolic acid) (PLGA). Original magnification ×200

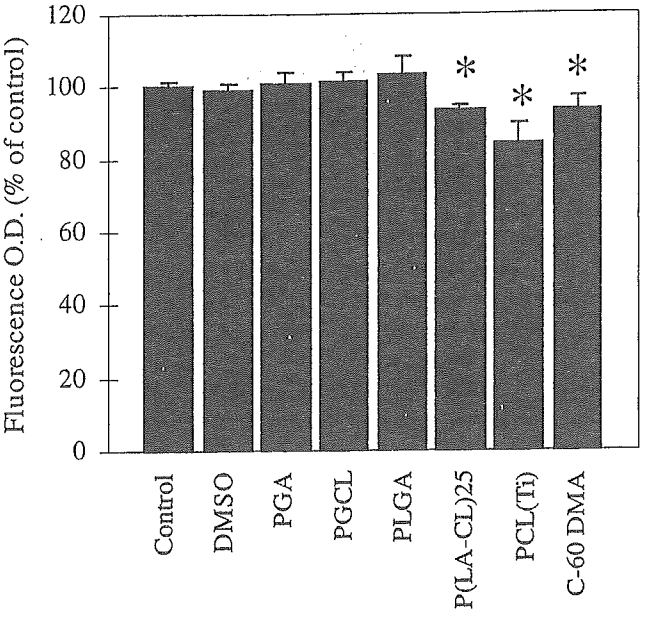

Fig. 2. Cell proliferation of human articular chondrocytes as determined by alamar blue assay after culturing with synthetic biodegradable polymers for 4 weeks. The proliferation in all samples exposed to dimethyl sulfoxide (*DMSO*) and biomaterials were calculated as a percentage of control values. *P(LA-CL)25*, poly(L-lactic acid-ε-caprolactone) 75:25 (w/w); *PCL(Ti)*, poly-ε-caprolactone (tetrabutoxy titanium); *C-60 DMA*, fullerene C-60 dimalonic acid. $*P < 0.05$ and *error bars* represent standard deviations of the mean

Results

Cell morphology

Cells were aggregated as high-density micromass cultures 2h after cell spotting. After 4 weeks of culture, the chondrocytes mainly formed a uniform sheet of chondrogenic cells with nodules. The cartilage nodules were first observed in the first week of the culture. These nodules were better visualized by staining the proteoglycans with alcian blue after 4 weeks of culture. The control cells showed less nodule formation and they were poorly defined (Fig. 1A). The cultures exposed to the PGA and PLGA had more distinct nodules and greater numbers of nodule formations than the controls (Figs. 1B and 1D). The nodules formed in the culture exposed to PGCL were less distinct and fewer in number than the nodules in the cultures exposed to PGA and PLGA, but were more distinct and numerous than the nodules of the control cultures (Fig. 1C). After alcian blue staining, light microscopic examination also revealed that PGA-, PGCL-, and PLGA-treated cultures contained denser extracellular matrix (ECM) than the controls. Cells extended from the edge of all micromass cultures, and the extending cells were spindle-shaped.

Cell proliferation assay

The proliferation rates of all the matrices are shown in Fig. 2, with error bars representing the standard deviation of the mean. All values for the samples exposed to the biomaterials were expressed as a percentage of the control average value, which was taken as 100%. The effect of DMSO on cell proliferation was not significant (99.3% ± 1.6%). The cell proliferations for PGA, PGCL, and PLGA were fairly parallel to that of control cell proliferation. The cell proliferation for P(LA-CL)25, PCL(Ti), and fullerene C-60 DMA were significantly inhibited compared to the control. The inhibitions for P(LA-CL)25 and fullerene C-60 DMA were mainly due to the small variation of the standard deviation. Despite being significantly different from the control, both proliferation values were fairly close to the control proliferation value.

Therefore, from the standpoint of cell proliferation, all materials except for PCL(Ti) remained viable candidates for tissue engineering. The values of cell proliferation for the samples exposed to PGA, PGCL, PLGA, P(LA-CL)25, PCL(Ti), and fullerene C-60 DMA were 101% ± 2.7%, 101.6% ± 2.2%, 103.5% ± 4.8%, 93.2% ± 1.4%, 84.3% ± 5.1%, and 93.6% ± 3.7%, respectively.

Proteoglycan synthesis

The proteoglycans bound with alcian blue were extracted with 4-M guanidine hydrochloride. Their levels were expressed as a percentage of the average control value, which was taken as 100% (Fig. 3). The intensity of alcian blue staining was found to be higher in PGA-, PGCL-, and PLGA-containing cultures than in the control culture. Among the biomaterials, PGA caused a significant 3.1-fold increase in cartilage proteoglycans compared to the control ($P < 0.05$). The samples exposed to PGCL (116.2% ± 10.1%) and PLGA (128.4% ± 11.1%) also produced

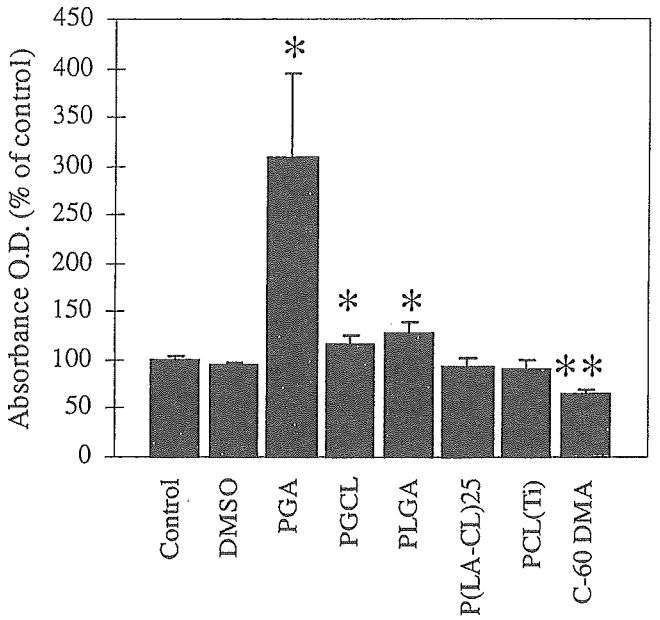

Fig. 3. Cartilage proteoglycan content of human articular chondrocytes as determined by the alcian blue staining method after culturing with synthetic biodegradable polymers for 4 weeks. The values are expressed as a percentage of control values. $^{*}P < 0.05$ and $^{**}P < 0.01$

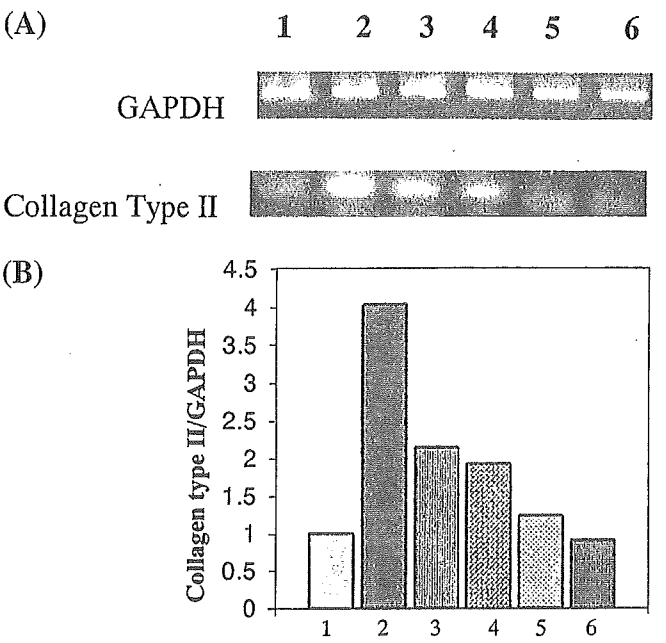

Fig. 4. Reverse transcription polymerase chain reaction (RT-PCR) analysis (**A**) and National Institutes of Health (NIH) image analysis quantitation of RT-PCR bands (**B**). In both figures, the level of collagen type-II gene expression was represented by the mRNA level of 4-week cultured human articular chondrocytes treated with different types of biodegradable polymers. The mRNA expression of housekeeping gene glyceraldehyde-3-phosphate dehydrogenase (*GAPDH*) was used for comparing the level of expression. **A** Lane 1, Control; lane 2, PGA; lane 3, PGCL; lane 4, PLGA; lane 5, P(LA-CL)25; lane 6, Fullerene C-60 DMA. **B** Bar 1, Control; bar 2, PGA; bar 3, PGCL; bar 4, PLGA; bar 5, P(LA-CL)25; bar 6, Fullerene C-60 DMA

significantly higher cartilage proteoglycans than the control. Copolymers P(LA-CL)25 (92.7% ± 10.5%) and PCL(Ti) (90.8% ± 9.1%) did not induce significant changes in cartilage proteoglycans compared to the control. Fullerene C60 DMA acted as a potent inhibitor (66.1% ± 4.7%) and caused a significant inhibition of cartilage proteoglycans ($P < 0.01$) compared to the control. The effect of DMSO (96% ± 1.1%) on cell differentiation was negligible.

Extracellular matrix gene expression

RT-PCR and corresponding National Institutes of Health (NIH) image analysis showed that all matrices consistently supported the expression of the collagen type II gene and that the PGA matrix had the strongest induction (Fig. 4). Slight increases in expression of the collagen type II gene were noted with PGCL, PLGA, and P(LA-CL)25 matrices. Expression of the collagen type II gene for fullerene C60 DMA was similar to the control. The PGA matrix also showed the strongest induction of the aggrecan gene (Fig. 5). Aggrecan gene expression was slightly increased in PGCL and PLGA matrices. The P(LA-CL)25 matrix caused an expression of this gene similar to that of the control, but the fullerene C60 DMA matrix caused decreased expression of this gene.

Expression of gap junction protein connexin 43 gene

To determine the expression of gap junctions during in vitro chondrocyte differentiation, RT-PCR and corresponding

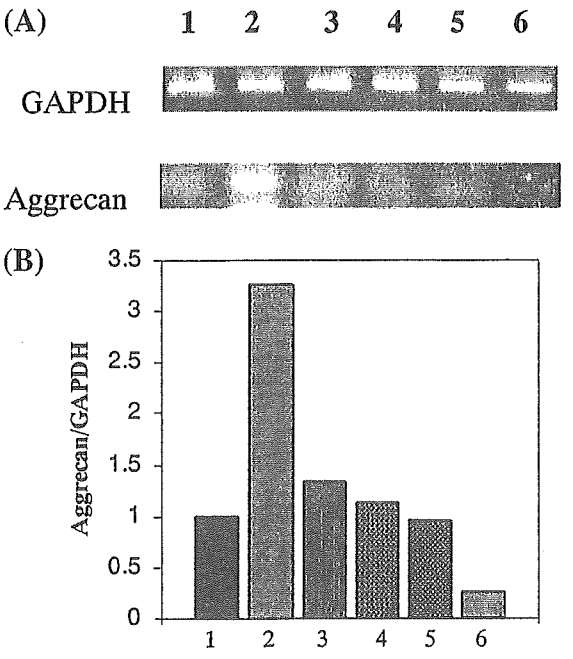

Fig. 5. RT-PCR analysis (**A**) and National Institutes of Health (NIH) image analysis quantitation of RT-PCR bands (**B**). In both figures, the level of aggrecan gene expression was represented by the mRNA level of 4-week cultured human articular chondrocytes treated with different types of biodegradable polymers. The mRNA expression of housekeeping gene GAPDH was used for comparing the levels of expression. *Lanes* and *bars* as defined in Fig. 4

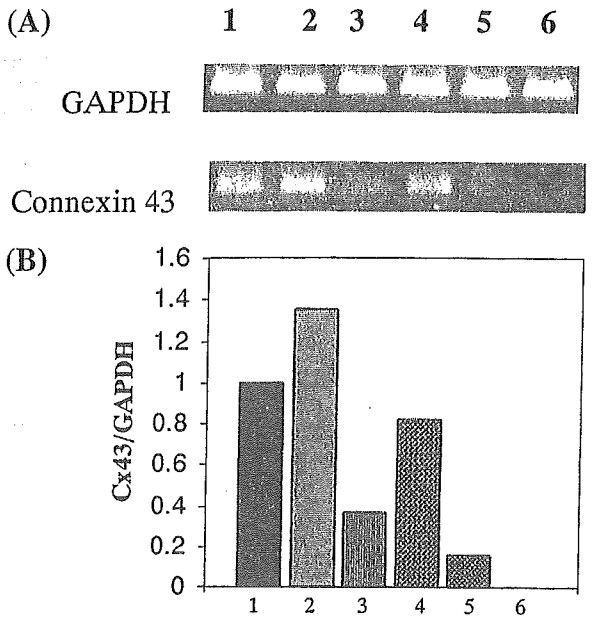

Fig. 6. RT-PCR analysis (**A**) and National Institutes of Health (NIH) image analysis quantitation of RT-PCR bands (**B**). In both figures, the level of connexin 43 gene expression was represented by the mRNA level of 4-week cultured human articular chondrocytes treated with different types of biodegradable polymers. The expression of GAPDH mRNA was used as an internal control. *Lanes* and *bars* as defined in Fig. 4

NIH image analysis was performed with connexin 43 in 4-week cultured human articular chondrocytes treated with various biodegradable biomaterials. Cx43 expression was normalized by comparison to the expression of GAPDH. Figure 6 shows that PGA induced the highest level of Cx43 mRNA expression, and a decreased level of expression was noted in the PLGA- and PGCL-treated cultures. A faint expression for P(LA-CL)25- and almost zero expression for fullerene C-60 DMA-treated cultures were observed.

Multiple regression analysis

Using multiple regression analysis, the correlation was investigated between cartilage proteoglycan production by the alcian blue method and the three gene expression levels. There was a high correlation between cartilage proteoglycan production and the three gene expression levels (data not shown).

Discussion

The evolution of new biodegradable polymers has drawn much attention in recent years, mainly because of growing application in clinical use. PCL is being utilized for biomedical applications such as controlled drug delivery systems[20] and also as surgical implants in rabbits.[21] Just as for PGA and PLLA, PCL degrades to a naturally occurring metabolite, 6-hydroxyhexanoic acid. To date, research to improve materials and the bioactivity of materials for tissue engineering has centered on PGA and PLLA; however, a short resorption time and low strength characteristics are two major drawbacks of these biodegradable materials. To widen the spectrum of biomaterial choices in tissue engineering, we investigated a copolymer of PGA and PCL, namely, PGCL, and copolymers of PLLA and PCL namely, P(LA-CL)25, PCL(Ti), and fullerene C60 DMA. To compare the bioactivity of these materials with commonly used materials, PGA and PLGA were included in this study. We also included PCL(Sn), synthesized using stannous 2-ethyl hexanoate as the catalyst, in our initial study, but following overnight culture after cell spotting, the cells were detached as a white condensed mass from 15 of 16 PCL(Sn)-coated glass wells in repeated studies. Therefore, PCL(Sn) was excluded from this study. Cells were also detached from 8 (50%) of a total of 16 glass wells coated with PCL(Ti). Thus, both PCL(Ti) and PCL(Sn) matrices were harmful to the cell attachment process. Decreased attachment of human articular chondrocytes with PCL matrix was previously reported.[22] After culture periods of 4 weeks, cell proliferation was significantly inhibited by the PCL(Ti) matrix, and together with its poor cell attachment ability, this ruled out PCL(Ti) as a matrix for future chondrocyte culture. The significant inhibition of cell proliferation by P(LA-CL)25 and fullerene C60 DMA matrices was a result of their narrow range of standard deviation, but, with proliferation levels of 93% of that for the control, they remain feasible candidates for tissue engineering biomaterials. Other matrices had comparable cell proliferation to the control.

During differentiation, chondrocytes secrete extracellular matrix (ECM) molecules characteristic of cartilage, such as type II collagen, aggrecan, and link protein, offering an environment that preserves the chondrocyte phenotype. Therefore, chondrocytes are defined both by their morphology and their ability to produce these characteristic ECM molecules. Collagen type II is regarded as the most important component among the ECM molecules. Previous study detected type II collagen as early as 7 days after beginning 3-D culture, and at 21 days, the matrix of the entire aggregate contained type II collagen.[23] Among the ECM molecules, aggrecan is a major proteoglycan.[24] It has been reported that in chick cartilage, aggrecan expression starts at embryonic day 5 in limb rudiments, continues through the entire period of chondrocyte development, and remains a biochemical marker of the cartilage phenotype thereafter.[25]

In this study, we demonstrated good cell differentiation with the formation of cartilaginous nodules on culture plates by alcian blue staining, which is commonly used for identification of cartilage, and by expression of ECM molecules collagen type II and aggrecan. The morphology after the designated culture period revealed that cells aggregated on the culture plate and formed cartilaginous nodules (Fig. 1). These nodules were first observed after 1 week of culture and progressively became denser as culture continued. These nodules contained copious amounts of ECM, which became stained intensely with alcian blue. The greatest cell

differentiation, a 3.1-fold increase of that of the controls, was found in the sample treated with PGA. The potencies of cell differentiation after 4 weeks of culture from the highest to the lowest were in the following order: PGA >> PLGA > PGCL > Control = DMSO > P(LA-CL)25 = PCL(Ti) >> fullerene C60 DMA. The increased cell differentiation with PGA and PLGA matrices are in agreement with our previous findings in a micromass culture system;[19] however, in our present study we included the matrix gene expression of these materials. The cell differentiation findings of PCL(Ti) and copolymers PGCL and P(LA-CL)25 could not be compared with other studies because we found no reports describing the effects of PCL and its associated polymers on chondrocyte differentiation. The recent discovery that fullerene C60 DMA can be produced in macroscopic quantities has sparked much interest in the chemistry of this unusual molecule, which did not cause acute toxic effects on mouse skin epidermis.[26] Increased cell proliferation and differentiation of rat embryonic limb bud cells by fullerene C60 were reported,[11] but the data of the present study showed that fullerene C60 DMA acted as a potent inhibitor of HAC differentiation.

As tissue engineering becomes increasingly complex, there is a need to understand how a specific biomaterial influences gene expression. Therefore, the matrices used in this study were evaluated with respect to their influence on the expression of collagen type II and aggrecan genes (Figs. 4 and 5). The increased expression of collagen type II and aggrecan genes in the PGA-, PGCL-, and PLGA-treated matrices was well correlated with their elevated level of cell differentiation values, as shown by alcian blue staining. The low expression of collagen type II and aggrecan genes in the fullerene C60 DMA-treated matrix paralleled the decreased level of cell differentiation, as shown by alcian blue. Therefore, low cell proliferation and differentiation values along with almost no expression of collagen type II and aggrecan genes in the fullerene C60 DMA-treated matrix completely exclude this matrix from use in ECM tissue engineering. The expression of collagen type II and aggrecan genes in the P(LA-CL)25-treated culture was consistent with its cell differentiation value. The data from this study showed that cultured chondrocytes also retained their phenotype throughout the experimental period, as indicated by expression of the type II collagen gene (Fig. 4A, 4B). To the best of our knowledge, this study is the first to show the bioactivity of PCL(Ti) and copolymers PGCL and P(LA-CL)25 in chondrogenic differentiation of HAC in a micromass culture system. Further, we know of no studies that have evaluated the matrix gene expression for PGA and PLGA matrices using HAC in a micromass culture system. Results of the present study confirmed PGA, PLGA, and PGCL as useful scaffolding matrices for cartilage tissue engineering, and information about the other matrices will further contribute to the development of improved cartilaginous constructs for future clinical implants.

The progression of chondrogenic differentiation can be followed by the expression of markers of cytodifferentiation. For example, precartilaginous condensations express type I collagen,[27] whereas the next phase of cartilage differentiation involves the expression of type II collagen, aggrecan, and link proteins, which form the cartilage matrix.[28] The mechanism of precartilaginous condensation is poorly understood, but cell–cell interactions are putative effectors for chondrocyte aggregation.[29] Chondrocytes in the primary culture can proceed through the same differentiation program as they do in the cartilaginous angle of the long bone, and the earliest morphological event on the way to overt differentiation is the formation of cell condensation.[17] The observed expression of Cx43 suggested that the process of condensation is in part caused by the interconnection of cells by means of gap junctions.[13] In this study, RT-PCR analysis showed that the mRNA level of Cx43 gene expression was consistent with chondrogenic differentiation in the presence of different biomaterials. Our findings on Cx43 expression by chondrocytes are in agreement with a previous study that reported expression of functional gap junctions by chondrocytes isolated from adult articular cartilage.[30] Gap junction-mediated intercellular communication is critically involved in the development of cartilage during differentiation.[31]

Conclusions

The analysis of three set of genes, namely collagen type II, aggrecan, and Cx43 was important to evaluate the effect of biodegradable polymers and other types of cartilaginous scaffolds on the chondrogenesis of HAC for tissue engineering.

Acknowledgments We are grateful for the support of Health and Labour Sciences Research Grants, and support from Research on Advanced Medical Technology, Ministry of Health, Labour and Welfare, and the Japan Health Sciences Foundation.

References

1. Taylor MS, Daniels AU, Andriano KP, Heller J. Six bioabsorbable polymers: in vitro acute toxicity of accumulated degradation products. J Appl Biomater 1994;5:151–157
2. Nakamura T, Shimizu Y, Okumura N, Matsui T, Hyon SH, Shimamoto T. Tumorigenicity of poly-L-lactide (PLLA) plates compared with medical-grade polyethylene. J Biomed Mater Res 1994;28:17–25
3. Matsusue Y, Yamamuro T, Oka M, Shikinami Y, Hyon SH, Ikada Y. In vitro and in vivo studies on bioabsorbable ultra-high-strength poly (L-lactide) rods. J Biomed Mater Res 1992;26:1553–1567
4. Furukawa T, Matsusue Y, Yasunaga T, Shikinami Y, Okuno M, Nakamura T. Biodegradation behavior of ultra-high-strength hydroxyapatite/poly (L-lactide) composite rods for internal fixation of bone fractures. Biomaterials 2000;21:889–898
5. Hope PG, Williamson DM, Coates CJ, Cole WG. Biodegradable pin fixation of elbow fractures in children. J Bone Joint Surg 1991;73:965–968
6. Kleinschmidt J, Marden L, Kent D, Quigley N, Hollinger J. A multiphase system bone implant for regenerating the calvaria. J Plast Reconstr Surg 1993;91:581–588
7. Hollinger JO. Preliminary report on the osteogenic potential of a biodegradable copolymer of polylactide (PLA) and polyglycolide (PGA). J Biomed Mater Res 1983;17:71–82

8. Tormala P, Pohjonen T, Rokkanen P. Bioabsorbable osteosynthetic implants of ultra-high-strength poly-L-lactide. A clinical study. Int Orthop 1996;20:392–394
9. Evans GR, Brandt K, Widmer MS, Lu L, Meszlenyi RK, Gupta PK, Mikos AG, Hodges J, Williams J, Gurlek A, Nabawi A, Lohman R, Patrick CW Jr. In vivo evaluation of poly (L-lactic acid) porous conduits for peripheral nerve regeneration. Biomaterials 1999;20:1109–1115
10. Hadlock T, Sundback C, Hunter D, Cheney M, Vacanti JP. A polymer foam conduit seeded with Schwann cells promotes guided peripheral nerve regeneration. Tissue Eng 2000;6:119–127
11. Tsuchiya T, Yamakoshi YN, Miyata N. A novel promoting action of fullerene C60 on the chondrogenesis in rat embryonic limb bud cell culture system. Biochem Biophys Res Commun 1995;206:885–894
12. Tsuchiya T, Oguri I, Yamakoshi YN, Miyata N. Novel harmful effects of [60] fullerene on mouse embryos in vitro and in vivo. FEBS Lett 1996;393:139–145
13. Kumar NM, Gilula NB. The gap junction communication channel. Cell 1996;84:381–388
14. Solursh M, Linsenmeyer TF, Jensen KL. Chondrogenesis from single limb mesenchyme cells. Dev Biol 1982;94:259–262
15. Willecke K, Hennemann H, Dahl E, Jungbluth S, Heynkes R. The diversity of connexin genes encoding gap junctional proteins. Eur J Cell Biol 1991;56:1–7
16. Schwab W, Hofer A, Kasper M. Immunohistochemical distribution of connexin 43 in the cartilage of rats and mice. Histochem J 1998;30:413–419
17. Loty S, Foll C, Forest N, Sautier JM. Association of enhanced expression of gap junctions with in vitro chondrogenic differentiation of rat nasal septal cartilage-released cells following their dedifferentiation and redifferentiation. Arch Oral Biol 2000;45:843–856
18. Okuda K, Hirota M, Hirobe T, Nagano M, Mochizuki M, Mashino T. Synthesis of various water-soluble C60 derivatives and their superoxide-quenching activity. Fullerene Sci Tech 2000;8:89–104
19. Rahman MS, Tsuchiya T. Enhancement of chondrogenic differentiation of human articular chondrocytes by biodegradable polymers. Tissue Eng 2001;7:781–790
20. Hombreiro PM, Zinutti C, Lamprecht A, Ubrich N, Astier A, Hoffman M, Bodmeier R, Maincent P. The preparation and evaluation of poly (epsilon-caprolactone) microparticles containing both a lipophilic and a hydrophilic drug. J Control Release 2000;65:429–438
21. Lowry KJ, Hamson KR, Bear L, Peng YB, Calaluce R, Evans ML, Allen WC. Polycaprolactone/glass bioabsorbable implant in a rabbit humerus fracture model J Biomed Mater Res 1997;36:536–541
22. Ishaug-Riley SL, Okun LE, Prado G, Applegate MA, Ratcliffe A. Human articular chondrocyte adhesion and proliferation on synthetic biodegradable polymer films. Biomaterials 1999;20:2245–2256
23. Johnstone B, Hering TM, Caplan AI, Goldberg VM, Yoo JU. In vitro chondrogenesis of bone marrow-derived mesenchymal progenitor cells. Exp Cell Res 1998;23:265–272
24. Watanabe H, Yamada Y, Kimata K. Roles of aggrecan, a large chondroitin sulfate proteoglycan, in cartilage structure and function. J Biochem (Tokyo) 1998;124:687–693
25. Schwartz NB, Domowicz M, Krueger RC Jr, Li H, Mangoura D. Brain aggrecan. Perspect Dev Neurobiol 1996;3:291–306
26. Nelson MA, Domann FE, Bowden GT, Hooser SB, Fernando Q, Carter DE. Effects of acute and subchronic exposure of topically applied fullerene extracts on the mouse skin. Toxicol Ind Health 1993;9:623–630
27. Langille RM, Solursh M. Formation of chondrous and osseous tissues in micromass cultures of rat frontonasal and mandibular ectomesenchyme. Differentiation 1990;44:197–206
28. Kosher RA, Gay SW, Kamanitz JR, Kulyk WM, Rodgers BJ, Sai S, Tanaka T, Tanzer ML. Cartilage proteoglycan core protein gene expression during limb cartilage differentiation. Dev Biol 1986;118:112–117
29. Frenz DA, Jaikaria NS, Newman SA. The mechanism.of precartilage mesenchymal condensation: a major role for interaction of the cell surface with the amino-terminal heparin-binding domain of fibronectin. Dev Biol 1989;136:97–103
30. Donahue HJ, Guilak F, Vander Molen MA, McLeod KJ, Rubin CT, Grande DA, Brink PR. Chondrocytes isolated from mature articular cartilage retain the capacity to form functional gap junctions. J Bone Miner Res 1995;10:1359–1364
31. Coelho CN, Kosher RA. Gap junctional communication during limb cartilage differentiation. Dev Biol 1991;144:47–53

Available online at www.sciencedirect.com
SCIENCE DIRECT®
Neuroscience Letters 370 (2004) 155–159
Neuroscience Letters
www.elsevier.com/locate/neulet

4-Hydroxynonenal modulates the long-term potentiation induced by L-type Ca^{2+} channel activation in the rat dentate gyrus in vitro

Tatsuhiro Akaishi[a,b], Ken Nakazawa[b], Kaoru Sato[b], Yasuo Ohno[b], Yoshihisa Ito[a,*]

[a] *Department of Pharmacology, College of Pharmacy, Nihon University, 7-7-1 Narashinodai, Funabashi-shi, Chiba 274-8555, Japan*
[b] *Division of Pharmacology, National Institute of Health Sciences, Setagaya-ku, Tokyo 158-8501, Japan*

Received 15 June 2004; received in revised form 23 July 2004; accepted 8 August 2004

Abstract

Increased oxyradical production and membrane lipid peroxidation (MLP) occur under physiological and degenerative conditions in neurons. We investigated whether 4-hydroxynonenal (4HN), one of the membrane lipid peroxidation products, affects long-term potentiation (LTP) in the rat dentate gyrus in vitro. Treatment of hippocampal slices with 4HN (10 μM) enhanced LTP without affecting basal evoked potentials. The enhancement was completely inhibited by 2 μM nifedipine, a blocker of L-type Ca^{2+} channels. In cultured dentate gyrus neurons, treatment of the cells with 4HN for 24 h resulted in a significant amount of cell death that was detoxified by glutathione, whereas short-term treatment with 4HN (≦6 h) had no effect. Nifedipine partially but significantly suppressed the 4HN-induced cell death. These results suggest that 4HN modulates LTP and induces delayed cell death through L-type Ca^{2+} channel activation in the dentate gyrus. 4HN thereby plays an important role in both physiological and pathophysiological events in the hippocampus.

Keywords: 4-Hydroxynonenal; Oxidative stress; Long-term potentiation; Ca^{2+} channel; Hippocampus; Dentate gyrus

Oxidative stress is implicated in a variety of physiological and pathophysiological processes such as immune defense, ischemia, and neurodegenerative diseases (e.g., Alzheimer's disease, AD) [7,8,17,23]. It has been shown that levels of membrane lipid peroxidation (MLP) and thiobarbituric-acid-reactive substances are elevated in AD brains [16,18]. Several reports have shown that one of the MLP products, 4-hydroxynonenal (4HN), is generated in response to oxidative insults and is found in association with many different neurodegenerative diseases, such as AD [14,17], Parkinson's disease [24], and sporadic amyotrophic lateral sclerosis [22]. We have recently reported that oxidative stress affects the activity of voltage-gated Ca^{2+} channels (VGCCs), and that the currents through VGCCs are significantly increased by treatment with 4HN in cultured dentate granule cells [1,2]. These results suggest that 4HN activates VGCCs in the dentate granule cells, and that this action is linked to both physiological and pathophysiological events.

Long-term potentiation (LTP) in the hippocampus is a form of synaptic plasticity and is thought to be one of the cellular mechanisms underlying learning and memory. LTP is induced by high-frequency stimulation (HFS), and it requires activation of *N*-methyl-D-aspartate (NMDA) receptors and consequent Ca^{2+} entry into the postsynaptic neurons at least in area CA1 of the hippocampus and the dentate gyrus [5]. Recent studies have demonstrated that not only Ca^{2+} influx through NMDA receptors, but also that through VGCCs or store-operated Ca^{2+} channels play important roles in the induction or regulation of LTP [4,6]. Recently, a link between oxidative stress and modulation of synaptic plasticity has been proposed. It has been demonstrated that physiologically relevant concentrations of hydrogen peroxide (H_2O_2), a membrane-permeable form of reactive oxygen species, modify synaptic plasticity in the hippocampal CA1 region in rats [13]. However, the involvement of 4HN in synaptic plasticity in the hippocampus has yet to be elucidated. To address this

* Corresponding author. Tel.: +81 474 65 5832; fax: +81 474 65 5832.
E-mail address: yoshiito@pha.nihon-u.ac.jp (Y. Ito).

0304-3940/$ – see front matter © 2004 Elsevier Ireland Ltd. All rights reserved.
doi:10.1016/j.neulet.2004.08.015

point, in the present study, the effects of 4HN on LTP in the rat dentate gyrus were examined in vitro. We found that 4HN modulates LTP via the activation of L-type VGCCs, and that long-term exposure of cultured dentate granule cells to 4HN induces neuronal death, at least in part, through mechanisms involving a VGCC-mediated pathway.

All procedures in this study were carried out in accordance with the guidelines of the National Institutes of Health Sciences. Preparation of hippocampal slices and recording of evoked potentials were done as described in our previous papers [3,12]. In brief, hippocampal slices (400 μm thick) were prepared from male Wistar rats (4–6 weeks old) and maintained in a chamber at 30 °C, where they were continuously perfused with oxygenated (95% O_2:5% CO_2) artificial cerebrospinal fluid (ACSF). The composition of the ACSF was as follows (in mM): 124 NaCl, 1.25 NaH_2PO_4, 2.5 KCl, 2.0 $CaCl_2$, 1.0 $MgCl_2$, 26.0 $NaHCO_3$, and 10.0 glucose. The perforant path was stimulated with a bipolar tungsten electrode, and the evoked potential was recorded extracellularly from the granule cell layer of the dentate gyrus with a glass capillary microelectrode filled with 2 M NaCl (tip resistance 2–8 MΩ). Single-pulse test stimulations (0.1 ms duration) were applied at 30-s intervals. The stimulus intensity was adjusted to produce synaptic potential amplitudes that were of 50% of the maximum.

Dentate gyrus neurons in the hippocampus were obtained from 3- to 4-day-old Wistar rats and enzymatically dissociated as described previously [1,2]. The cells were suspended in a mixture of 50% Neurobasal medium containing 2% B-27 supplement, 73 μg/ml L-glutamine, and 50% astrocyte-conditioned medium (ACM). The cells were plated on polyethyleneimine-coated 96-well plates (20,000 cells/cm^2). The ACM-containing medium was changed to an ACM-free medium 1 day after the plating. The culture medium was changed twice a week thereafter. At days 7–8, the medium was removed and replaced with Locke's solution (154 mM NaCl, 5.6 mM KCl, 2.3 mM $CaCl_2$, 1.0 mM $MgCl_2$, 3.6 mM $NaHCO_3$, 10 mM glucose, and 5 mM 4-(2-hydroxyethyl)-1-piperazineethanesulfonic acid; pH 7.2). The effects of 4HN on LTP or cell viability were investigated using drugs added to ACSF or Locke's solution, respectively. 4HN (Cayman Chemical, Ann arbor, MI, U.S.A.) and nifedipine (Sigma, St Louis, MO, U.S.A.) were prepared as 1000× and 500× stock solutions, respectively in ethanol. Glutathione (GSH)-ethyl ester (Sigma) was prepared as a 100× stock solution in saline. Cell viability was evaluated by the 3-(4,5-dimethythiazol-2-yl)-2,5-diphenyltetrazolium bromide (MTT) reduction assay, as described previously [11,14].

To evaluate changes in evoked potentials, the amplitude of the population spike (PS) was measured as described in our previous reports [3,12]. When 10 μM 4HN was applied to the slices, there was no change in PS amplitude (Fig. 1A), suggesting that 4HN does not affect basal evoked potentials in the dentate gurus. We next investigated effects of 4HN on LTP in the dentate gyrus. In control slices, the application of HFS produced a robust potentiation of the PS that

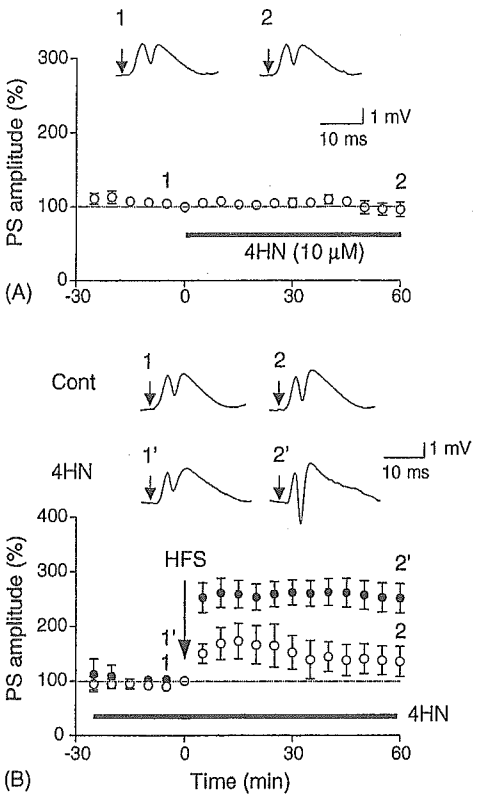

Fig. 1. Effects of 4HN on basal evoked potentials and LTP in the dentate gyrus in vitro. (A) Time-course of changes in basal evoked potentials ($n = 4$). Hippocampal slices were treated with 4HN (10 μM) for 60 min (0–60 min), and evoked potentials were observed without applying HFS. (B) Time-course of LTP induced in the absence (open circles, $n = 4$) or presence (closed circles, $n = 6$) of 4HN (10 μM). HFS (100 pulses at 100 Hz) was applied at time 0. The amplitude of the evoked potentials is expressed as a percentage of the baseline value (at time 0), which was recorded immediately before the application of 4HN (A) or HFS (B). Insets are representative records of evoked potentials at the times denoted by the numbers. A test stimulation was delivered at the times indicated by arrows. All data are presented as the mean ± S.E.M.

lasted for 60 min and reached approximately 140% of the basal level (Fig. 1B, open circles). When hippocampal slices were pretreated with 10 μM 4HN for 1 h, the degree of LTP that was then induced was larger than in the control group (Fig. 1B). The mean amplitude of PS of 30–60 min after HFS was 139.1 ± 28.6% in the control group and 258.0 ± 25.5% in the 4HN-treated group. We have shown recently, using the whole cell patch clamp technique, that 4HN selectively activates L-type VGCCs in dentate granule cells [2]. In order to examine whether VGCCs contribute to the 4HN-induced enhancement of LTP, we investigated the effects of nifedipine, an L-type VGCC blocker. In our preliminary experiment, exposure of slices to nifedipine (2 μM) alone did not affect LTP ($n = 4$, data not shown). As shown in Fig. 2, the 4HN-induced enhancement of LTP was completely blocked when slices were treated with 2 μM nifedipine. These results suggest that 4HN enhances LTP in the dentate gyrus, and that this enhancement is attributable to the activation of L-type VGCCs.

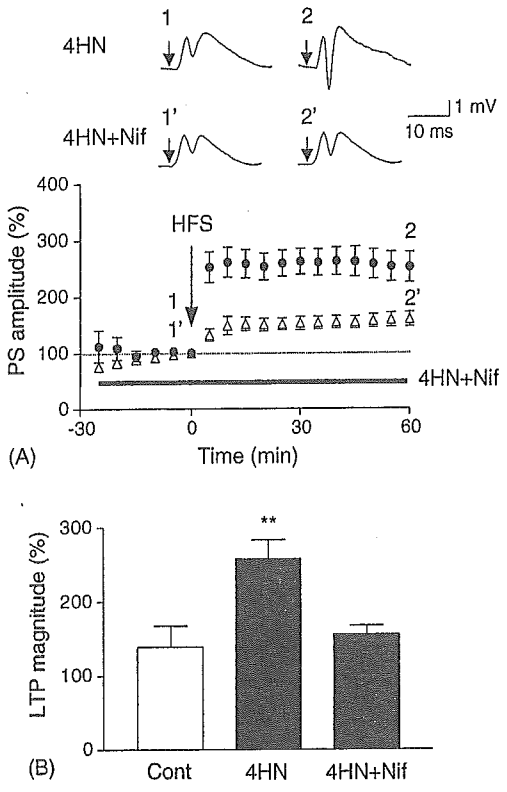

Fig. 2. Effects of nifedipine (Nif) on the enhancement of LTP in the dentate gyrus in vitro. (A) Time-course of changes in evoked potentials. Hippocampal slices were treated with 4HN (10 μM) in the presence or absence of Nif (2 μM) for 1 h, and then HFS was applied at time 0 (open triangles, $n = 6$). The amplitude of the evoked potentials is expressed as a percentage of the baseline value, which was recorded immediately before the onset of HFS (time 0). Insets are representative records of evoked potentials at the times denoted by the numbers. A test stimulation was delivered at the times indicated by arrows. To allow a direct comparison, the 4HN-treated data (the same data as Fig. 1B) are superimposed. (B) Comparison of LTP magnitude among the three groups (control group, Cont; 4HN-treated group, 4HN; 4HN- and Nif-cotreated group, 4HN + Nif). The average of evoked potential amplitudes 30–60 min after HFS was calculated as an index of LTP magnitude. Values are given as the mean ± S.E.M. $^{**}P < 0.01$ vs. Cont, Dunnett's test.

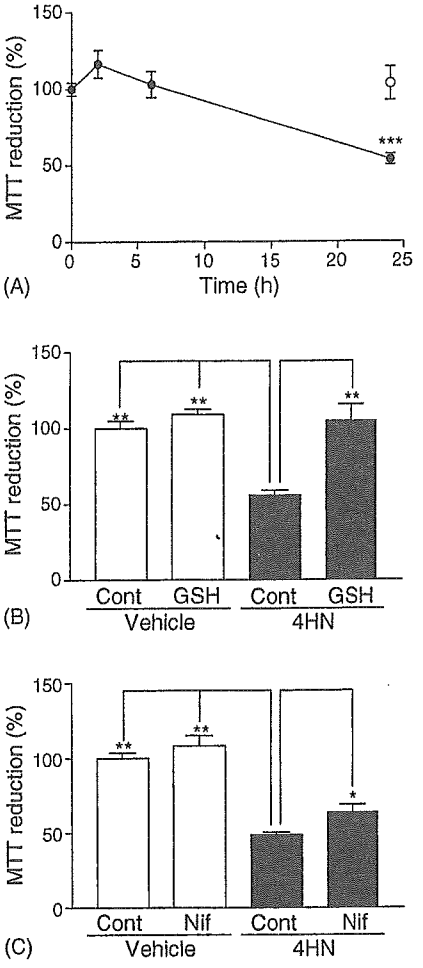

Fig. 3. 4HN induces delayed cell death in dentate gyrus neurons, but this effect is inhibited by simultaneous treatment with either GSH or Nif. (A) Time-course of changes in 4HN-induced cell death. 4HN (10 μM) was applied at time 0, and levels of MTT reduction were examined at the time point indicated (closed circles, $n = 6$–8). To enable a direct comparison, the vehicle (0.02% ethanol)-treated cells are shown as ○ ($n = 7$). GSH-ethyl ester (1 mM) blocked (B, $n = 7$–9), and Nif (2 μM) attenuated (C, $n = 10$–14) the delayed cell death induced by 4HN. Cells were exposed to the indicated agents, and neuronal survival was quantified. Values are presented as the mean ± S.E.M. $^{***}P < 0.001$ vs. the vehicle, Student's t-test. $^{*}P < 0.05$; $^{**}P < 0.01$ vs. 4HN (Cont), Dunnett's test.

There is a growing body of evidence to suggest that prolonged exposure of hippocampal neurons to 4HN results in delayed cell death [10,14,15]. Therefore, we also examined the effects of 4HN on cell viability using primary dentate gyrus neurons. The time course of 4HN-induced toxicity is shown in Fig. 3A. Exposure of the cells to 10 μM 4HN resulted in no decrease in the levels of MTT reduction during the first 6 h. In contrast, a significant decrease in MTT levels was observed at 24 h following the application of 4HN (53.9% of basal levels). The level of MTT reduction in the 4HN-treated groups was significantly lower than in the vehicle-treated groups (Fig. 3A). GSH is a covalent modifier of 4HN and can thereby detoxify 4HN [1,15]. We examined the effects of GSH-ethyl ester, a membrane-permeable form of GSH, on 4HN-induced cell death. As shown in Fig. 3B, the 4HN-induced cell death was completely blocked when cells were treated with 1 mM GSH-ethyl ester. In addition, nifedipine (2 μM) partially but significantly attenuated 4HN-induced cell death (Fig. 3C), indicating that Ca^{2+} influx through VGCCs, at least in part, underlies the cell death.

The data presented here demonstrate that 10 μM 4HN significantly enhances LTP without affecting basal evoked potentials in the dentate gyrus, and that this enhancement is completely blocked when slices are treated with 2 μM nifedipine. These findings suggest that Ca^{2+} influx through the L-type VGCCs plays a pivotal role in synaptic plasticity in certain conditions in the dentate gyrus. To our knowledge, this is the first report to provide direct evidence that 4HN modulates LTP via the activation of L-type VGCCs. However, it

remains to be elucidated whether the 4HN-induced enhancement of LTP is involved in physiological and/or pathophysiological phenomena.

In general, MLP products are thought to be involved in certain types of neurodegenerative disorders. For example, levels of 4HN are increased in association with the neurodegenerative process in postmortem tissue samples from patients with AD [16]. Studies of experimental models of AD suggested a pivotal role for 4HN in the neurodegenerative process [11,14,15]. It has been reported that age-related changes in the levels of MLP in the hippocampus are associated with alterations in the level of LTP in the dentate gyrus [19]. On the other hand, there are recent indications supporting the involvement of MLP in physiological phenomena. It has been reported that levels of MLP increase in response to stimuli that induce LTP [21]. Kamsler and Segal [13] demonstrated that a physiologically relevant concentration (1 μM) of H_2O_2 increased LTP and suppressed long-term depression, while higher concentrations (0.5–5 mM) of H_2O_2 suppressed basal synaptic transmission in the rat hippocampus. In our previous experiments using the whole cell patch clamp technique, we demonstrated that low concentrations (1 and 10 μM) of H_2O_2 and 4HN selectively modulate L-type VGCCs in cultured dentate granule cells [1,2]. Because it has been already shown that VGCCs are involved in various physiological functions in neurons [9,20], the action of 4HN as well as H_2O_2 may be implicated not only in pathophysiological phenomena but also in physiological events in the hippocampus. In the present study, we used a concentration of 10 μM throughout the electrophysiological experiments because 10 μM 4HN showed a robust and significant VGCC-enhancing effect in our previous report [2]. Further detailed investigations using various concentrations of 4HN will be necessary to elucidate the relevance of 4HN to physiological phenomena in the hippocampus.

In the present study, we have also demonstrated that long-term exposure of cultured dentate gyrus neurons to 4HN, at a concentration that is known to modulate the activity of L-type VGCCs [2], results in a decrease of cell viability. It is not clear, at present, how long-term exposure to 4HN could induce cell death in these neurons. A possible explanation is that excessive Ca^{2+} influx through VGCCs contributes to neuronal death, although these channels are also involved in various physiological functions in these neurons. Long-term exposure of 4HN may switch on arrays of toxic events through excessive Ca^{2+} influx, while its short-term exposure may lead to physiological functions including the enhancement of LTP.

The exact mechanisms whereby 4HN modulates the VGCCs activity in neurons remain to be elucidated. In our preliminary studies, enhancement of Ca^{2+} current by 4HN requires a lag time period of about 1 h to become evident. The modulatory effect of 4HN on LTP and cell death, as shown in the present study, may be mediated through several kinase- or phosphatase-dependent pathways.

Acknowledgments

This work was partly supported by Health and Labour Science Research Grants for Research on Advanced Medical Technology from the Ministry of Health, Labour, and Welfare, Japan, a Grant-in-aid for Scientific Research from the Ministry of Education, Culture, Sports, Science, and Technology, Japan (KAKENHI 13672319) awarded to K.N., and a Grant-in-aid for Young Scientists from the Ministry of Education, Science, Sports, and Culture, Japan (KAKENHI 15700280) awarded to K.S.

References

[1] T. Akaishi, K. Nakazawa, K. Sato, H. Saito, Y. Ohno, Y. Ito, Hydrogen peroxide modulates whole cell Ca^{2+} currents through L-type channels in cultured rat dentate granule cells, Neurosci. Lett. 356 (2004) 25–28.

[2] T. Akaishi, K. Nakazawa, K. Sato, H. Saito, Y. Ohno, Y. Ito, Modulation of voltage-gated Ca^{2+} current by 4-hydroxynonenal in dentate granule cells, Biol. Pharm. Bull. 27 (2004) 174–179.

[3] T. Akaishi, H. Saito, Y. Ito, K. Ishige, Y. Ikegaya, Morphine augments excitatory synaptic transmission in the dentate gyrus through GABAergic disinhibition, Neurosci. Res. 38 (2000) 357–363.

[4] A. Baba, T. Yasui, S. Fujisawa, R.X. Yamada, M.K. Yamada, N. Nishiyama, N. Matsuki, Y. Ikegaya, Activity-evoked capacitative Ca^{2+} entry: implications in synaptic plasticity, J. Neurosci. 23 (2003) 7737–7741.

[5] T.V.P. Bliss, G.L. Collingridge, A synaptic model of memory: long-term potentiation in the hippocampus, Nature 361 (1993) 31–39.

[6] L.M. Grover, T.J. Teyler, Two components of long-term potentiation induced by different patterns of afferent activation, Nature 347 (1990) 477–479.

[7] K. Ishige, Q. Chen, Y. Sagara, D. Schubert, The activation of dopamine D4 receptors inhibits oxidative stress-induced nerve cell death, J. Neurosci. 21 (2001) 6069–6076.

[8] K. Ishige, D. Schubert, Y. Sagara, Flavonoids protect neuronal cells from oxidative stress by three distinct mechanisms, Free Radic. Biol. Med. 30 (2001) 433–446.

[9] K. Ito, K. Nakazawa, S. Koizumi, M. Liu, K. Takeuchi, T. Hashimoto, Y. Ohno, K. Inoue, Inhibition by antipsychotic drugs of L-type Ca^{2+} channel current in PC1 cells, Eur. J. Pharmacol. 314 (1996) 143–150.

[10] Y. Ito, M. Arakawa, K. Ishige, H. Fukuda, Comparative study of survival signal withdrawal- and 4-hydroxynonenal-induced cell death in cerebellar granule cells, Neurosci. Res. 35 (1999) 321–327.

[11] Y. Ito, Y. Kosuge, T. Sakikubo, K. Horie, N. Ishikawa, N. Obokata, E. Yokoyama, K. Yamashina, M. Yamamoto, H. Saito, M. Arakawa, K. Ishige, Protective effect of *S*-allyl-L-cysteine, a garlic compound, on amyloid β-protein-induced cell death in nerve growth factor-differentiated PC12 cells, Neurosci. Res. 46 (2003) 119–125.

[12] Y. Ito, K. Tabata, M. Makimura, H. Fukuda, Acute and chronic intracerebroventricular morphine infusions affect long-term potentiation differently in the lateral perforant path, Pharmacol. Biochem. Behav. 70 (2001) 353–358.

[13] A. Kamsler, M. Segal, Hydrogen peroxide modulation of synaptic plasticity, J. Neurosci. 23 (2003) 269–276.

[14] Y. Kosuge, Y. Koen, K. Ishige, K. Minami, H. Urasawa, H. Saito, Y. Ito, *S*-Allyl-L-cysteine selectively protects cultured rat hippocampal neurons from amyloid β-protein- and tunicamycin-induced neuronal death, Neuroscience 122 (2003) 885–895.

[15] I. Kruman, A.J. Bruce-Keller, D. Bredesen, G. Waeg, M.P. Mattson, Evidence that 4-hydroxynonenal mediates oxidative stress-induced neuronal apoptosis, J. Neurosci. 17 (1997) 5089–5100.
[16] M.A. Lovell, W.D. Ehmann, M.P. Mattson, W.R. Markesbery, Elevated 4-hydroxynonenal in ventricular fluid in Alzheimer's disease, Neurobiol. Aging 18 (1997) 457–461.
[17] R.J. Mark, E.M. Blanc, M.P. Mattson, Amyloid β-peptide and oxidative cellular injury in Alzheimer's disease, Mol. Neurobiol. 12 (1996) 211–224.
[18] S. Miranda, C. Opazo, L.F. Larrondo, F.J. Munoz, F. Ruiz, F. Leighton, N.C. Inestrosa, The role of oxidative stress in the toxicity induced by amyloid β-peptide in Alzheimer's disease, Prog. Neurobiol. 62 (2000) 633–648.
[19] C.A. Murray, M.A. Lynch, Dietary supplementation with vitamin E reverses the age-related deficit in long-term potentiation in dentate gyrus, J. Biol. Chem. 273 (1998) 12161–12168.
[20] Y. Niikura, K. Abe, M. Misawa, Involvement of L-type Ca^{2+} channels in the induction of long-term potentiation in the basolateral amygdala-dentate gyrus pathway of anesthetized rats, Brain Res. 1017 (2004) 218–221.
[21] N.S. Nilova, L.N. Polezhaeva, Peroxidative oxidation of lipids in slices of olfactory cortex of the rat brain during long-term potentiation, Neurosci. Behav. Physiol. 26 (1996) 23–26.
[22] W.A. Pedersen, W. Fu, J.N. Keller, W.R. Markesbery, S. Appel, R.G. Smith, E. Kasarskis, M.P. Mattson, Protein modification by the lipid peroxidation product 4-hydroxynonenal in the spinal cords of amyotrophic lateral sclerosis patients, Ann. Neurol. 44 (1998) 819–824.
[23] Y. Sagara, K. Ishige, C. Tsai, P. Maher, Tyrphostins protect neuronal cells from oxidative stress, J. Biol. Chem. 277 (2002) 36204–36215.
[24] A. Yoritaka, N. Hattori, K. Uchida, M. Tanaka, E.R. Stadtman, Y. Mizuno, Immunohistochemical detection of 4-hydroxynonenal protein adducts in Parkinson disease, Proc. Natl. Acad. Sci. U.S.A. 93 (1996) 2696–2701.

Available online at www.sciencedirect.com

SCIENCE DIRECT®

ELSEVIER

European Journal of Pharmacology 495 (2004) 27–33

www.elsevier.com/locate/ejphar

Desensitization of $P2X_2$ receptor/channel pore mutants

Ken Nakazawa[a,b,*], Yasuo Ohno[b]

[a] *Molecular and Cellular Pharmacology Section, National Institute of Health Sciences, 1-18-1 Kamiyoga, Setagaya, Tokyo 158-8501, Japan*
[b] *Division of Pharmacology, National Institute of Health Sciences, 1-18-1 Kamiyoga, Setagaya, Tokyo 158-8501, Japan*

Received 8 January 2004; received in revised form 10 May 2004; accepted 12 May 2004

Abstract

Properties of five mutants of $P2X_2$ receptor/channel having amino acid residue-substitution at the pore region were examined by expressing the channels in *Xenopus* oocytes. When the concentration–response relationship for ATP-evoked current was obtained, the current amplitude was increased along with the concentrations of ATP for the wild type channel whereas the amplitude was rather decreased with highest concentrations for four of the five mutants as if an "inactivation-like" mechanism occurs to these mutants. Upon a long exposure (30 s) to ATP, time-dependent decay in the ATP-evoked current was observed for three of the five mutants, suggesting that desensitization occurs to these mutants. The time course of the desensitization was well fitted with a single exponential time whereas that of the recovery from the desensitization could be better fitted with multiple exponentials than with a single exponential. The relationship between the desensitization and the "inactivation-like" mechanism was discussed.

Keywords: $P2X_2$ receptor; Channel pore mutant; Desensitization; ATP responsiveness

1. Introduction

When appropriate stimulation (change in membrane potential or ligand-binding) is given, voltage- and ligand-gated ion channels, respectively, exhibit transition from closed state to open state. In a number of channels, opened channels gradually shut even if the stimulation continues. This phenomenon is called "inactivation" for voltage-gated channels (Hodgkin and Huxley, 1952; Hille, 1992a), and generally called "desensitization" for ligand-gated channels (Katz and Thesleff, 1957; Hille, 1992b). The desensitization was also found for ion channels gated by extracellular ATP (P2X receptor/channels; see reviews, Ralevic and Burnstock, 1998; Khakh, 2001; North, 2002). Among P2X receptor/channel subclasses, $P2X_1$ and $P2X_3$ receptor/channels exhibit marked desensitization whereas the $P2X_2$ receptor/channel does not exhibit desensitization when expressed as homomeric channels.

We previously utilized channel pore mutants of $P2X_2$ receptors to determine factors contributing to the potency of multivalent cation block (Nakazawa et al., 2002). In the present study, we studied the dependence of the current permeating through these pore mutants on ATP concentrations, and the kinetics of the current during a long exposure to ATP. We found an "inactivation-like" phenomenon in the concentration–response study and desensitization in the kinetic study. The time courses of the desensitization and recovery from the desensitization were analyzed, and the relation between the desensitization and the "inactivation-like phenomenon was discussed using possible schematic models.

2. Materials and methods

2.1. Ionic current measurement

Mutants of $P2X_2$ receptor constructed from the cloned rat $P2X_2$ receptor (Brake et al., 1994) used in this study were those described by Nakazawa et al. (2002). The substitutions applied to the mutants were Asn^{333} to alanine (N333A), Thr^{336} to alanine (T336A), Leu^{338} to alanine (L338A), Gly^{342} to alanine (G342A) and Asp^{349} to asparagine (D349N). Channels were expressed in *Xenopus* oocytes and ionic currents permeating through them were measured

* Corresponding author. Tel.: +81-3-3700-9704; fax: +81-3-3707-6950.
E-mail address: nakazawa@nihs.go.jp (K. Nakazawa).

0014-2999/$ - see front matter © 2004 Elsevier B.V. All rights reserved.
doi:10.1016/j.ejphar.2004.05.021